Large Area Protein Patterning Reveals Nanoscale Control of Focal Adhesion Development

ARTICLE *in* NANO LETTERS · FEBRUARY 2010

Impact Factor: 13.59 · DOI: 10.1021/nl903875r · Source: PubMed

NANO LETTERS

pubs.acs.org/NanoLett

Large Area Protein Patterning Reveals Nanoscale Control of Focal Adhesion Development

Jenny Malmström,[†] Brian Christensen,[‡] Hans P. Jakobsen,[†] Jette Lovmand,[†,‡] Rasmus Foldbjerg,[§] Esben S. Sørensen,[‡] and Duncan S. Sutherland*[,†]

[†]Interdisciplinary Nanoscience Center (iNANO), [‡]Department of Molecular Biology, [§]Department of Environmental and Occupational Medicine, and Aarhus University, Denmark

ABSTRACT Focal adhesion development in cells adherent to surface bound fibronectin presented as 200, 500, or 1000 nm diameter circular patches or as homogeneous controls is studied by fluorescence and scanning electron microscopy. Fundamental cellular processes such as adhesion, spreading, focal adhesion and stress fiber formation are shown to be dependent on the spatial distribution of ligands at this scale. Large area samples enable the study of whole cell populations and opens for new potential applications.

KEYWORDS Protein nanopatterns, focal adhesion, colloidal lithography, cell adhesion, fibronectin

Most mammalian cells are dependent on adhering to the extracellular matrix (ECM) and/or neighboring cells. Therefore cell adhesion plays a pivotal role in many biological processes such as guidance of cells during embryonic development, wound repair, as well as serving as a signal transduction pathway for extracellular signals.[1,2] Cells adhere to the ECM through cell surface receptors, mainly integrins that are heterodimeric transmembrane proteins.[1] Integrins serve as a signal transduction pathway influencing a range of processes in the cell.[3,4] To form a stable focal adhesion (FA) integrins cluster together and assemble a number of proteins on the intracellular side (e.g., vinculin and paxillin) that in turn connect to the actin skeleton of the cell.[1,2,5,6] Focal adhesions have been reported to be of the size scale from 1 to 10 μm[1,6] whereas nascent adhesions/focal complexes have been detected as small complexes down to 100 nm.[2] These complexes normally form in motile or spreading cells under the lamellopodia as the membrane is moving forward and the actin network in the lamellopodia is moving backwards.[2] The nascent adhesions/focal complexes are typically transient and under normal conditions either disassemble or transform into mature rod-shaped focal adhesions at the boundary between the lamellopodia and the lamella. The focal adhesions are characterised by the inclusion of at least one new protein (zyxin) and a connection to actin fibers.[2] The mature focal adhesions are believed to be under a continuous pulling force from the actin stress fibers and their growth regulates the assembly of the system. During the transition from focal complexes to mature focal adhesions, the early focal adhesions are thought to experience forces from both the actin polymerisation in the lamellopodium and the newly forming actin fiber.[2] The extracellular matrix is organized on the nanoscale[7] and integrin clustering on the nanoscale has been shown to be important to events such as focal adhesion assembly, cell spreading, and migration[8−14] It has been shown that integrin ligands (RGD peptides) with a spacing over 73 nm does not support focal adhesion formation and cell spreading.[8,9] On a larger scale, micropatterning of cell adhesive regions have shown to influence cell survival,[15] cell shape and alignment,[15−18] adhesion strength,[19] and differentiation.[20] Aiming to investigate the minimal size of a focal adhesion that supports cell adhesion and/or spreading the submicrometer size is interesting. Lehnert et al[21] have utilized microcontact printing to achieve square fibronectin patterns with side lengths of 0.3−3 μm and interestingly found that cells could not spread on patches smaller than 0.1 μm^2 if spaced 5 μm apart. Pesen et al[22] produce circular or ringshaped fibronectin patterns using electron beam lithography suggesting a lower limit of adhesive ligands required for focal adhesion formation. These findings are supported by Slater et al[23] that produce fibronectin patterns of 90−400 nm (however of varying geometry) where adhesion size and proliferation was affected. Arnold et al[11] utilize a combination of electron beam lithography and micellar lithography producing adhesive patches of RGD peptides with side lengths ranging from 100 nm to 3000 nm where cells showed tendency to bridge between adjacent domains for patterns below 500 nm in order to adhere. These studies verify the importance of further studies of cell adhesion to ECM ligands clustered at this size scale.

In this study we develop a robust route to patterning protein patches over large areas in the 100 nm−1000 nm range by a simple extension of colloidal lithography and

* To whom correspondence should be addressed. E-mail: duncan@inano.dk.
[||] Author e-mail address: (J.M.) jennym@inano.dk.
Received for review: 11/19/2009
Published on Web: 00/00/0000

DOI: 10.1021/nl903875r | *Nano Lett.* **XXXX,** *xxx,* 000-000

utilize it to study the interaction of cells with extracellular matrix components laterally organised at the nanometer scale. We make use of the large patterned areas (tens of cm^2 per process) to carry out these studies on whole cell populations that have not previously been performed via the small area patterning approaches. In our system we have studied the adhesion, morphology, and spreading of a model cell line to fibronectin nanopatterns targeting specifically the weaker adhesive interactions expected for cells at these interfaces, utilizing a defined and soft cell rinsing protocol based on density lift-off. Making use of a combination of fluorescence microscopy and scanning electron microscopy we correlate cellular adhesion to patch size. We observe that cell attachment occurs already from small ECM patches (from 200 nm) and the level of interaction in terms of first localization of focal adhesion complexes (from 500 nm) and then connection to defined actin filaments (from 1000 nm) is controlled by the size of the fibronectin patch. This approach demonstrates a route to a detailed control of the level of cellular adhesion via a geometric parameter for whole cell populations. A large area production of patterned ECM ligands opens for systematic studies of for example cell differentiation and can also provide sufficient material to measure molecules excreted from the cells, but most importantly it provides a more physiologically relevant system that takes the inherent variation in the population of cultured cells into account.

Our approach to protein patterning utilizes a nanoscale chemical contrast of patches of gold in a background of silicon dioxide fabricated via colloidal lithography. Silicon wafer substrates, precoated in a 4 nm Ti and 30 nm Au layer by sputter deposition, were cleaned in solvents and UV ozone before use. Colloidal monolayer masks of dispersed particles were formed by an electrostatic self assembly approach reported previously[24] depositing sequential layers of PDDA (poly(diallyldimethylammonium chloride), PSS (poly(sodium-4-styrenesulfonate), and polyaluminium chloride followed by assembly of a short range ordered array colloidal mask. Mask assembly is carried out from dilute colloid solutions in deionized water that are then dried and applied to later pattern transfer under vacuum conditions. A significant limitation of this approach is that the mask pattern formed can easily be lost as result of particle clustering in response to capillary forces arising during the drying process. For smaller particles (<150 nm), this can be prevented by controlling the surface wettability and charge. For larger particles, it has been addressed by the coadsorption of smaller particles to minimize lateral particle motion;[24] however these smaller particles make the masks unsuitable for most pattern transfer steps. An alternative approach makes use of heating of the adsorbed polymer particles close to their glass transition to increase their contact area to immobilize the particles. For larger polystyrene particles, heating up to 100°C is not sufficient to stabilize the particles against capillary forces. In addition, larger area patterning ($1-10\ cm^2$) is complicated by the formation of gas bubbles at the surface leading to large defects. We introduce a simple and robust solution by carrying out a thermal treatment in a custom-built sealed pressure chamber, which prevents gas formation while allowing heating of water above 100°C. This simple alternative step allows us to create dispersed colloidal patterns routinely over tens of cm^2 for particles up to several micrometers in diameter and opens the way to study for example molecular events occurring in cells over the 100−1000 nm range. Colloidal mask assembly was made from aqueous solutions of 100, 200, 500, and 1000 nm particles. The pattern of the colloidal mask is transferred to the substrate by deposition of a 1 nmTi/12 nmSiO_2 layer by physical vapor deposition and a lift off step utilizing tape striping or sonication of the colloidal particles. Residues of colloidal particles left after particle stripping are removed by oxygen plasma or UV/ozone treatment. The generated short range ordered arrays of gold patches in a silicon dioxide background are then used for chemical functionalization by the approach as reported previously[25] to create protein adhesive domains in a polyethylene oxide-based protein rejecting background. In brief, the gold regions of the surface are modified by octadecylmercaptane and the whole surface is coated with PLL(20)-g[3.5]-PEG(2). A subsequent immersion in fibronectin solutions generates a protein nanopattern where the PLL-g-PEG coating on SiO_2 prevents protein binding while protein binds to the hydrophobic surface regions. A further blocking step with BSA was carried out before cell experiments. We have previously studied this functionalization extensively generating ∼100 nm protein nanopatterns.[25,26] The overall process is schematically outlined in Figure 1a and Figure 1 b shows SEM images of 100, 200, 500, and 1000 nm patches with the brighter gold regions showing up. The attachment and spreading of a mammalian breast cancer cell line (MDA-MB-435 cells, 20h adhesion) onto fibronectin presented as nanopatterns with systematically varied protein patch size was studied and compared to fibronectin homogeneous controls or homogeneous or nanopatterned BSA. We used a mild rinsing protocol, utilizing density lift-off, aiming to study a wide range of adhesion strengths likely to be present in particular on the smaller protein patches, and quantified cell adhesion and cell area using fluorescence microscopy.

We have previously shown that protein nanopatterning utilizing protein adsorption to hydrophobic gold, in contrast to PLL-g-PEG adsorption onto SiO_2, provides robust protein patterns.[25,26] The detailed interaction of the cells in this study were investigated using SEM, providing evidence that they preferentially contact the protein patches. In addition, very few cells attached on the negative control (PLL-g-PEG on SiO_2 exposed to fibronectin) and those that did attach were round. Thus, the cells are restricted to attach to the protein patches and these are spaced far enough apart (>70 nm[8]) that integrins binding to FN on adjacent patches cannot directly assemble in the same focal complex. This leads to

DOI: 10.1021/nl903875r | *Nano Lett.* **XXXX,** *xxx,* 000-000

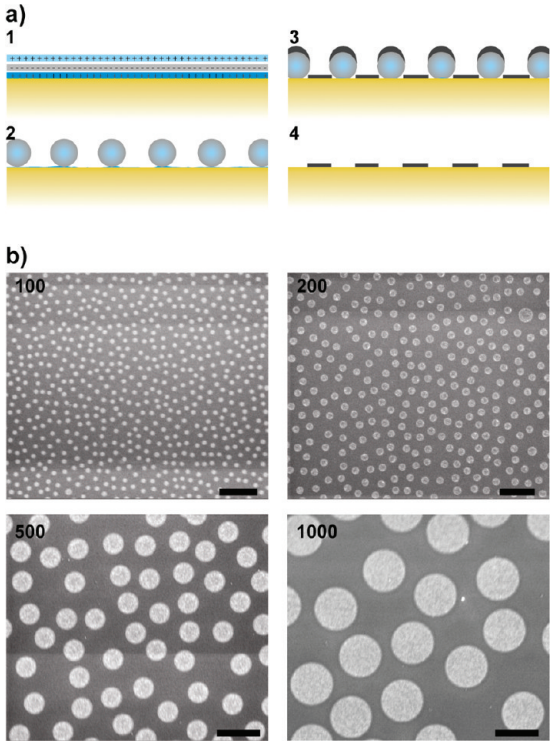

FIGURE 1. (a) Illustration showing steps involved in the nanofabrication. (a-1) Deposition of three polyelectrolyte layers gives the surface a positively charge. (a-2) Assembly of polystyrene particles forms array with short range order. After the deposition of particles they are heated in a custom build pressure chamber leading to stronger surface interaction whereby ordered arrays of large particles can be achieved. (a-3) Evaporation of material and subsequent lift-off gives the final result (a-4) of gold holes in a SiO_2 background where the SiO_2 can be rendered protein rejecting using PLL-g-PEG, thus leading to the production of protein nanopatterns. (b) SEM images of 100−1000 nm gold holes (bright) in SiO_2 film. Scalebar 1 μm.

a system where a limited number of integrins in each adhesion spot is generated by the underlying pattern geometry allowing the exploration of effects on attachment and cell morphology. Integrin clustering is an early event in the onset of focal complex/adhesion formation and once integrins are clustered the intracellular assembly of focal adhesion proteins build up.[1] Arnold et al.[8] have established a maximum distance for single integrins to be regarded as clustered by the cell whereas we focus on how many clustered integrins (number or area) are needed to assemble intracellular focal adhesion proteins.

Figure 2 shows representative fluorescence images of cells stained for the actin cytoskeleton bound to 200 nm, 500 nm, 1000 nm, and homogeneous hydrophobic surfaces. A large number of cells are bound to each surface type, which reflects the soft rinse protocol utilized with both spread and round cells observed on each of the surface types. A clear difference in the proportion of round cells at each of the surface types is observed. While the majority of the cells at the 200 nm surface appear round, an increasing proportion of spread cells are seen on the 500 nm, 1000 nm, and homogeneous surfaces, respectively. In addition, the

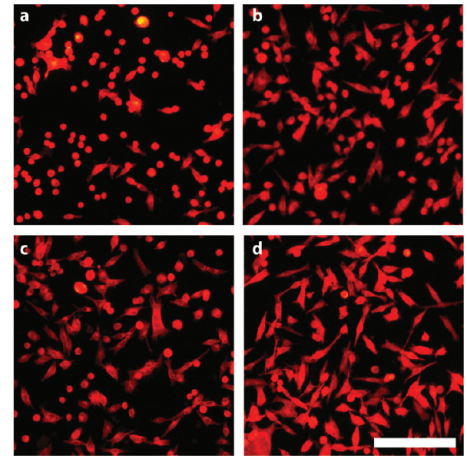

FIGURE 2. Representative microscopy pictures cells with rhodamine labelled actin adhering to fibronectin patterns of (a) 200 nm, (b) 500 nm and (c)1000 nm or (d) homogenous control. Images display one-fourth of a field of view using 10× objective. Scalebar 200 μm.

spread cells on the homogeneous surface appear to be larger compared the other surfaces. We have quantified the cell number, average spread area, and the proportion of spread cells at each of the surface types that are displayed in Figure 3. The cell number observed at the 200 nm surface is significantly lower than the other surfaces (Figure 3a). The number of cells adhering to the 500 and 1000 nm surfaces are somewhat larger than that on the homogeneous surface, however, while this was significant in this study it was not shown to be significantly larger in the full repeated experiment. The lower cell number at the 200 nm surface correlates to a much lower proportion of spread cells compared to the other surfaces (Figure 3b). We have rigorously scored cells as round only if they do not show any membrane protrusion or lamellipodia interacting with the surface in order to distinguish between cells showing some level of interaction and no interaction. We equate the round cells with weakly adherent cells. We have carried out a parallel study utilizing bovine serum albumin nanopatches as a control study (shown in the Supporting Information with cell number quantified in Figure S1 and representative fluorescence microscope images in Figure S2). All the cells adhering to the BSA-coated nanopatterns were entirely round showing no significant interaction with the surfaces. We attribute the observed binding of these cells to the surfaces to the density lift-off rinse protocol which was originally reported for the study of weak cell to protein interactions.[27] Our study is carried out after 20 hours of attachment time so we do not expect these cells to spread further. The proportion of spread cells on the nanopatterned fibronectin is substantially higher for the 500 nm surface, compared to the 200 nm, and then increases further for the 1000 nm and the homogeneous surface (Figure 3b). These data reflect only the shape of the cells, however the round cells are substantially smaller than the spread cells. The average spread area of the cells (Figure 3c) reflects this change in proportion of round cells with an

DOI: 10.1021/nl903875r | *Nano Lett.* **XXXX,** *xxx,* 000-000

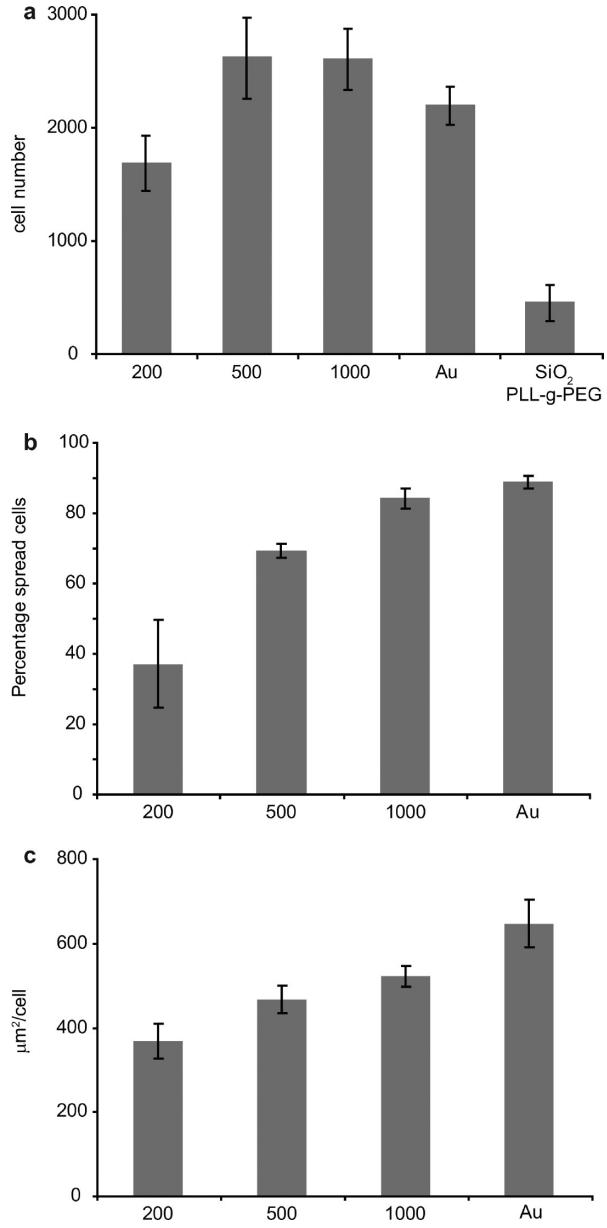

FIGURE 3. (a) Cell adhesion at fibronectin presented at homogenous interface and as nanopatterns of 200, 500, or 1000 nm patches after 20 h presented as average cell number with standard error mean per sample (three fields of view (1.5 mm^2) with 10× objective counted per sample, $n = 4$). (b) Percentage of spread cells calculated from one sample per condition (3 images) presented as average and standard deviation and (c) area per cell presented as an average with standard deviation.

increasing average spread area from 200 to 500 to 1000 nm. The homogeneous surface shows a substantially larger average spread area than the 1000 nm surface despite similar proportion of spread cells which demonstrates quantitatively the larger size of the spread cells observed on the homogeneous surfaces (Figure 2d - for full frame images separated into nucleus, actin and vinculin see Supporting Information Figure S3).

The larger proportion of round cells at the smaller patch sizes indicates that the cells are less able to interact with these patches. To investigate how the cells interact with the surface we utilized higher magnification fluorescence microscopy (×63) and stained the actin skeleton, the nucleus and for the focal complex/focal adhesion associated protein vinculin. Figure 4 displays representative images of cells at the different fibronectin surfaces. For each surface an overlay of actin (red), vinculin (green), and the nucleus (blue) is shown as well as separate images for actin and vinculin and a zoom of a region of the vinculin stained image. Cells on 200 nm fibronectin patches (Figure 4a-d) are in general not very spread (Figures 2a and 3b,c) and in most cases devoid of well-defined vinculin spots or clear actin filaments. Some granularity and small and faint spots can be seen in vinculin stained images (Figure 4c) in the outer region of the membrane and in lamellipodia (example in Figure 4d). Focal complexes or nascent adhesions of sizes down to 100 nm[28] have been observed mainly in the lamellipodia of spreading cells. These complexes are thought to be transient structures that can transform into focal adhesions at the lamella edge and maturing to link to the actin stress fibers.[2] Here we observe significant levels of cellular adhesion (Figures 2a and 3a) and a proportion of the cells are able to spread (Figures 2a and 3b,c) and form small vinculin staining complexes resembling these early adhesion complexes after 20 hours in culture (Figure 4d) on surfaces which limit the regions of extracellular contact to 200 nm patches. Focal complexes/nascent adhesions are thought to be transient; here the formation of larger complexes would require the bridging of several fibronectin patches, so it maybe that focal complexes are prevented from transforming in focal adhesions at such ECM patterns. Cells on 500 nm fibronectin patches (Figures 2b and 4e−h) are significantly more spread than on the 200 nm patches. Cells on this surface also exhibit mainly small less-defined vinculin spots and few actin filaments, however, a few more-defined and elliptically shaped but still small vinculin spots are observed linking to thin actin filaments.

For the biggest protein patches (1000 nm) almost all the cells are spread (Figures 2c and 4i−l) and exhibit many well-defined vinculin localizations. Although the cells are still largely devoid of thick actin stress fibers, a significant number of the vinculin spots are elongated and colocalized to the end of thin actin fibers. To some extent for the 500 nm patches, and to a larger extent for the 1000 nm patches, more defined vinculin spots are observed underneath the cell body in addition to the small complexes seen at the periphery of the cell membrane. We postulate that these defined spots are small focal adhesions as opposed to focal complexes observed on the smaller patches. On the homogenous control (Figures 2d and 4m−p) the cells have well-defined, comparatively large and rod-shaped mature focal adhesions that in many cases are connected to thick actin stress fibers. The strong mechanical contacts to the surface and well-defined cytoskeleton correlates to the larger spread area per cell observed compared to the 1000 nm patch

DOI: 10.1021/nl903875r | *Nano Lett.* **XXXX,** *xxx,* 000-000

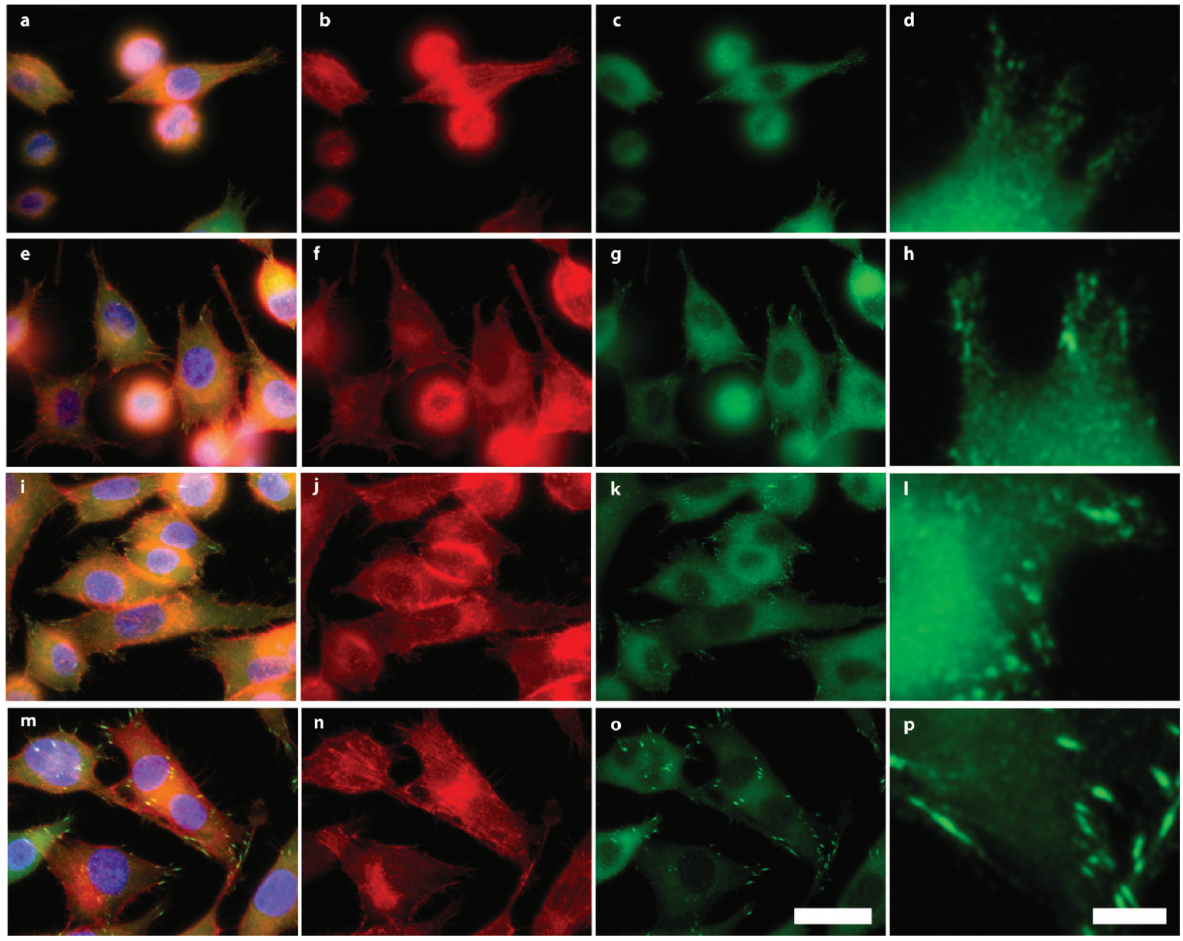

FIGURE 4. Representative microscopy pictures displaying one-fourth of a field of view using a 63× objective showing (from left to right) overlay of red staining actin, green staining vinculin, and blue staining the nucleus, separate views of actin and vinculin, and a zoom of a representative region of the vinculin image. (a−d) 200 nm patches, (e−h) 500 nm, (i−l) 1000 nm and (m−p) homogenous control. Scalebar 30 μm (5 μm for zoom).

surface (Figure 3b) and fits with the expectations for cells adhering to fibronectin at rigid homogenous 2D substrates.[29] The focal adhesions observed at the 1000 and 500 nm patches that are linked to the cytoskeleton show a more round morphology or an extended shape formed from several round structures compared to the rod shapes on the homogeneous surface. We have quantified the length and aspect ratio of the vinculin spots on the different protein patterns and homogeneous surface that are tabulated in the Supporting Information (Table S2). The length of the vinculin spots on the different samples appears to reflect the underlying fibronectin distribution. While for the homogenous surfaces they are around 2 micrometers in length with an aspect ratio of ∼2.7, they become 1.3 micrometers in length on the 1000 nm patterns with an aspect ratio around ∼2.0. The optical-based resolution of our microscope would lead to a systematic overestimation of the size of length and width of the structures and a measured 1.3 micrometer length would be expected for a structure limited to a 1 micrometer patch. The vinculin spots at the 500 nm pattern surface are seen to be ∼0.9 micrometers long with a calculated aspect ratio of ∼1.6. The aspect ratio for these small structures is not possible to measure accurately as a result of the limited optical resolution; it is however clearly larger than 1. Again the 0.9 μm measured length is that expected from a structure limited to the 500 nm pattern. For the 200 nm patterns the vinculin spots are below the limit that the microscope can quantify (as seen by the significant reduction in the measured polydispersity of sizes) but are seen to be small (<0.8 μm) with no obvious assymetry. The size of and distance between the round vinculin spots appears to correlate well with the underlying nanopattern. While the 200 nm and 500 nm patches are not visible in the light microscope images, with differential interference contrast (DIC) mode we observe the 1000 nm structures around the cells. We have used merged fluorescence and DIC images from the periphery of the cells to compare the location of vinculin spots and the fibronectin patches.

Figure 5a shows a membrane extension in the foreground with the vinculin (green) image overlaid on a DIC image. The nanostructured surface can be seen in the background (from

DOI: 10.1021/nl903875r | *Nano Lett.* **XXXX,** *xxx,* 000-000

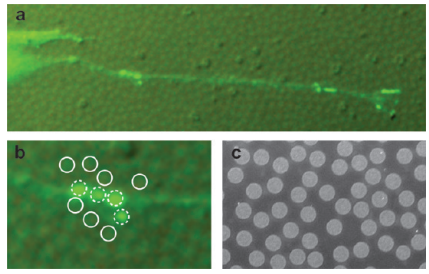

FIGURE 5. (a) Zoom of part of a cell adhering to 1000 nm fibronectin patches stained green for vinculin overlayed on the DIC image where the nanostructures are visible. Green fluorescent vinculin spots can be seen in the retraction fibre and at closer inspection in panel b the correlation of the focal contacts to the fibronectin patches is indicated. Positions of fibronectin nanopatches are indicated by solid circles outside the cell extension and dotted circles underneath. An SEM image of similar magnification is displayed in c for comparison of the pattern geometry.

the DIC image only, not present in green fluorescent image). The overall shape and size of the vinculin spots appears to fit with the underlying nanopattern (Figure 5a). In a zoom shown in Figure 5b, we have indicated the location and approximate size of the protein patches with circles (solid circles are outside the cell extension and clearly visible, the broken circles are of patches that lie under the cell membrane). This pattern fits very well to the characteristic distribution of the protein patches (Figure 5c shows an SEM image of a 1000 nm patch substrate without cells with approximately matched magnification). This provides strong evidence that these vinculin spots localize to the underlying fibronectin patches. On the nanopatterned surfaces, we observe adhesive complexes at the periphery of the cells and have utilized SEM of fixed and dried cells to investigate these regions of the cells simultaneously with the underlying nanopattern distribution. Figure 6 displays images of cells adhering to the different surfaces (200 nm a,b, 500 nm c,d, 1000 nm e,f, and homogenous control g,h). Two images at different magnification are presented for each substrate. The left panel displays the lower magnification (scalebar 5 μm) and the right panel displays a higher magnification (scalebar 2 μm). In both cases, only small parts of cells are imaged and the resolution is much greater than that can be achieved with optical microscopy. Membrane protrusions can be seen extending from the cell body in all images and they appear to be of similar sizes regardless of the underlying surface pattern. We identify a majority of these cell extensions as retraction fibers present in motile cells.[30,31] These retraction fibers appear at least to scale with the smallest structures (200 nm) and do not obviously follow the protein patches on that surface type. For the bigger nanopatches, the retraction fibers are seen to often preferentially follow, and/or locate the end of the fibre to the protein nanopatches. Obviously a cell is in constant change and thus the retraction fibers cannot be expected to end at protein patches at all times. In Figure 6d (500 nm), it can be seen how the retraction fibers branch and change direction to locate to the protein patches. Some retraction fibers also have some

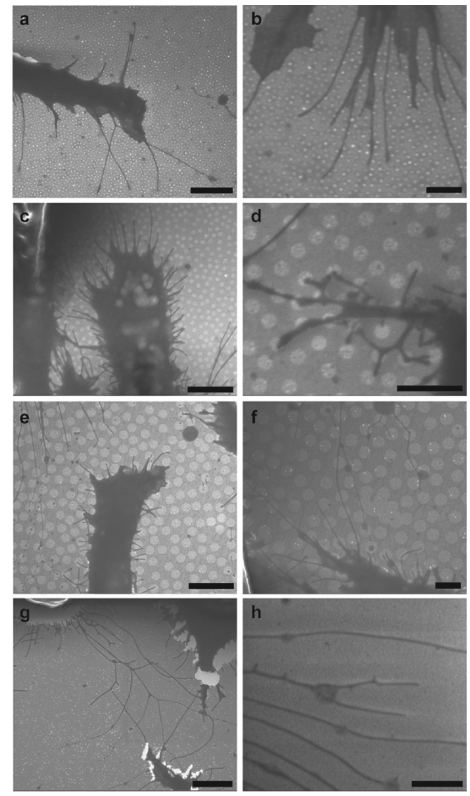

FIGURE 6. SEM images of cells adhering to FN adsorbed at the different substrates. Cells on 200 nm protein patches are displayed in a,b, 500 nm in c,d, and 1000 nm in e,f. Panels g,h show cells adhering to the homogenous control. Two different images with different magnifications are shown for each condition with the lower magnification in the left panel (scalebar 5 μm) and the higher magnification in the right panel (scalebar 2 μm).

thicker parts, like beads on a string, and in Figure 6e,f these beads can be observed mainly on the protein patches. While focal complexes/nascent adhesions typically form under the lamellipodia they may form in retraction fibers[32] and we interpret these beads as distinct contact points to the surface and postulate that they may be short-lived focal complexes. The size of them appears (as the retraction fibers) to be largely independent of the underlying surface and may thus be a fundamental minimal size required by the cell. In rare cases, these structures were also observed on the 200 nm patch size, there having to extend over several nanopatches at once, whereas the bead structures are somewhat smaller than and fit nicely on the 1000 nm patches. If this is a fundamental size of a focal complex needed for the cell to spread, that provides a likely explanation to why the cells show poor adhesion and spreading on the 200 nm protein patches. On the homogenous control, the cells can be seen breaking off from the surface. This is interpreted as an effect of the force applied during the critical point drying of the cells being larger than the hydrophobic interactions binding the fibronectin to the surface.

We have studied the effect of the variation in ligand patch size on cell attachment and morphology of a model cell line and demonstrate a systematic change of cell behaviour. The

DOI: 10.1021/nl903875r | *Nano Lett.* **XXXX,** *xxx,* 000-000

spread cells show long retraction fibers when imaged by SEM indicating that they may be motile. Significant adhesion and a limited proportion of spread cells are seen on the 200 nm patches (0.03 μm^2) and show small vinculin localizations in the outer cell membrane similar to nascent adhesions/focal complexes in spreading cells. At 500 nm (0.2 μm^2) the majority of cells are spread, displaying focal complex structures and in addition a small number of small but elliptical focal adhesions linked to thin actin fibers. With increase of patch size to 1000 nm (0.8 μm^2) the cells develop significant numbers of these small but elongated focal adhesions linked to actin fibers and in addition a few larger focal adhesions that appear to bridge several adhesive patches. The cell morphology is distinctly different from that at the flat rigid homogeneous surface where substantially more spreading is observed and long rodlike focal adhesions linked to thick actins stress fibers. The different morphology of the cells on the nanopatterns compared to the homogenous substrate is similar to that observed for cells adhering to fibronectin adsorbed at a range of soft materials.[33,34] It appears that the micrometer and submicrometer patterns of the ECM ligand are able to limit the length of the developing focal adhesions to single patches altering the cells ability to generate force and to spread and move. In addition, we believe that the size of the focal complexes that can form and grow is limited by the patch size. Since stress appears to be exerted on these complexes by the actin polymerisation,[2] the level of stress that these focal complexes can sustain, and their growth in response to it, may be altered at nanopatterned surfaces which would have impact on cell spreading and motility.

Other studies have investigated cell adhesion to adhesive regions of a similar size range fabricated by other means. Lehnert et al.[21] generated an array of different sized nanopatterns of fibronectin over a range of patch sizes and allowed the cells to sample all the patterns together. They observe that cells adhere and spread on substrates with an adhesive area of down to 0.1 μm^2. Slater et al[23] investigated smaller adhesive regions in a similar approach to this study where the cells cannot choose between different surface structures. They utilize Nanosphere Lithography that generates triangular nano/microstructures of local order over larger areas but with substantial variation in the geometry and orientation of the different nanostructures and in addition with defects over the larger scale. They suggest that a different behavior (cell spreading) starts at adhesive patches of 0.04−0.1 μm^2 and above. Our system can be described as a disordered array with local short range order and being very homogenous over larger scales. The details of the order of the display of nanoscale signals to cells has recently been shown to be of importance in characterising cellular responses[10,35] Arnold et al[11] showed, utilizing hierarchical patterns of peptide-based integrin ligands, that a minimal number of six single integrin attachment sites are needed to support focal adhesion and that cells were able to bridge adjacent adhesive domains along the same actin bundle if the separation was lower than 500 nm, leading to synergistic adhesion strengthening. The global density of fibronectin is lower on the nanopatterned substrates than the homogenous control, and the surface area available for protein binding is also varying for the different nanopatterned substrates (∼15% for 100 nm, ∼20% for 200 nm, ∼25% for 500 nm, and ∼35% for 1000 nm). This may be a contributing factor to the results, however it is acknowledged that the local density of integrin ligands is an important parameter for cell spreading,[21,23] rather than the global density. Lehnert et al[21] propose however that the total area of high local density ligand is of importance in generating a sufficient response of second messengers in the cell and found a critical coverage of 15% adhesive area. In our study, we address protein patterns of varying size where the global fibronectin coverage is high, but where the patch spacing is small (<300 nm). This patch spacing is in the regime where cells adhering to peptide nanopatterns have been shown to bridge paxillin domains between neighboring patches.[11]

We show many defined focal adhesions for FN area of 0.8 μm^2 but only few at 0.2 μm^2. In contrast, Lehnert et al[21] showed for their smallest dot sizes of 0.1 μm^2 that their cells still behaved as on the homogenous control for center to center spacing of 2μm. Our results from 500 nm patches (0.2 μm^2) supports this finding in that the cells spread, however we find only a low level of defined focal contacts and no defined stress fibers in cells attaching to this surface. As we go further down in size than Lehnert et al,[21] we also find that for the relatively small interpatch distances used in our study (<300 nm) an adhesive area of 0.03 μm^2 (200 nm in diameter) impairs the possibility of the cells to spread and to form focal adhesions. Furthermore, we have previously shown that even smaller adhesive islands of 100 nm in diameter significantly reduces cell adhesion, down to the level of that on the negative control (SiO_2 PLL-g-PEG).[36] These findings were confirmed in this study as well with exclusively round and very few adherent cells on adhesive patches of ∼100 nm in diameter (samples were included for SEM imaging, data not shown). On the basis of our results we propose that an adhesive area of 0.03 μm^2 (200 nm in diameter) is around the lowest limit to cluster enough integrins to form focal complex/nascent adhesions and/or to go above threshold for intracellular signalling molecules leading to spreading of the cells, whereas 0.008 μm^2 (100 nm in diameter) does not support cell adhesion at all. Contrasting these results to those of Arnold et al,[11] it appears that the cells cannot readily achieve bridging and synergistic adhesion strengthening on our substrates of 100 and 200 nm in diameter patches if at all they allow for integrin clustering (wall to wall distance of 100 nm patches is ∼100 nm and for 200 nm patches it is ∼160 nm). The wall to wall distance between the 500 nm patches is ∼230 nm while that of the 1000 nm is ∼290 nm (see Supporting Information Table S1). We observe examples of bridging across between 1000 nm patches and only rarely between 500 nm patches,

DOI: 10.1021/nl903875r | *Nano Lett.* **XXXX,** *xxx,* 000-000

which suggests that for these protein ligand nanopatterns the size of the nanopattern is relevant for the ability to bridge across between adhesive patches.

The transition between focal complexes and focal adhesions is not well understood at the molecular level but is thought to be dependent on, or at least strongly promoted by, mechanical force, typically leading to elongation of the focal adhesion into a rodlike morphology.[2] We form our protein patterns on rigid base substrates. Cell adhesion to homogenous fibronectin coating on these substrates leads to well-defined actin stress fibers and mature focal adhesions presumably as a result of large mechanical forces in the actin fibers that can be generated at the unyielding substrates. The limitation of the focal complexes to small regions (200−500 nm) while apparently allowing the formation of small focal complexes reminiscent of the nascent adhesions observed at the leading edge of spreading cells, does not allow the transition to larger mature focal adhesions linked to actin fibers. These are observations made across a whole cell population after 20 hours in culture. The transition between focal complexes and focal adhesions can apparently progress on peptide ligand arrays by bridging across between small adhesive sites.[11] We do not readily observe these several micrometer long focal adhesions until on the 1000 nm patches. This difference in adhesion development on our fibronectin nanopatterns compared to peptide arrays[11] may result from the different binding mechanisms occurring. Two significant differences may occur. Fibronectin displays several binding motifs and can interact with a wide range of integrins.[1,37] We carried out a RGD peptide block for homogeneous and 1000 nm patch surfaces and show a significant but only partial blocking (see Supporting Information Figure S4). This nicely demonstrates that RGD based integrin binding is only a proportion of the adhesive ability of ECM proteins such as fibronectin and highlights the importance of carrying out protein-based patterning studies in addition to peptide based studies. A second significant difference lies in the characterization of the rigidity of the surface. Our protein patches are formed on rigid substrates but the fibronectin layer adds an important level of softness in the interaction. Fibronectin has been widely studied in vitro as a mechnosensitive element and is shown to unfold domains in response to mechanical force.[38] The process of transformation between focal complexes and adhesions is thought to involve the level of force applied from the actin matrix.[2,39] By limiting the size of the adhesive patch one presumably limits the level of force than can be applied to one patch. To generate more force may require then bridging to another patch. There may be significant differences in the response of protein and peptide patches in that fibronectin patches may be able to regulate the level of force by unfolding. These differences may explain the fact that we do not observe bridging between closely separated protein patches that was observed on similar sizes and spacing of peptide patches.[11]

We propose that the size of the protein patches limits the conversion of focal complexes to focal adhesions, perhaps by limiting the force that can be applied, and for the patch sizes in the 200−500 nm range, leading to the adhesive complexes being arrested at the stage of focal complexes. For patch sizes of 500 nm, some transformations to focal adhesions occur which remain submicrometer, but for 1000 nm patches the formation of micrometer length focal adhesions and connection to actin fibers can occur on a regular basis. However the thickness and presumably the force that can be exerted on these focal adhesions is limited, and only small numbers of long rodlike focal adhesions bridging several patches are observed. The morphology and adhesion complexes of cells adhering to our protein patterns resembles that for cells adhering to materials of intermediate softness.[33,34] These functional coatings, while on rigid substrates, maybe able to act like soft materials in terms of the forces that can be generated in the actin filaments.

Our results present the potential for giving defined surface cues to cellular systems. There is a large body of work from us and others focused on utilizing nanoscale and microscale topography to give signals to cells.[17,18,40,41] This is in part resulting from the ease to produce large areas of substrates for these studies, which has not yet been commonplace in nanopatterning of proteins for cell studies. Screening a range of materials has lead to substantial advances in surface mediated signals to cells, allowing for control of adhesion, proliferation, signalling,[40] and differentiation.[35] However there is still a lack of an in depth understanding of mechanistically how these signals are communicated to the cells. Our approach allows us to work with cell populations, rather than with individual cells, while still controlling the lateral organization of the ECM at the nanoscale. This provides a more physiologically relevant system that takes the inherent variation in the population of cultured cells into account. Our large scale approach is robust and does not require expensive lithography or deposition equipment making it easily applicable and will have significant impact both on understanding the importance of ECM organization at nanostructured materials and in developing new and more specific surface signals to induce specific cell differentiation in the area of stem cell culture, tissue engineering, and biomaterials.

Acknowledgment. We thank Jacques Chevallier and Folmer Lyckegaard for their input on the fabrication process as well as kindly performing sputtering and evaporation. This work was funded through the Lundbeck Foundation and Danish research council (645-05-0016 and 274-08-0464)

Supporting Information Available. Detailed experimental procedures, cell adhesion data to BSA, full field of view microscopy pictures and data from RGD-block experiment. This material is available free of charge via the Internet at http://pubs.acs.org.

DOI: 10.1021/nl903875r | *Nano Lett.* **XXXX,** *xxx,* 000-000

REFERENCES AND NOTES

(1) Geiger, B.; Bershadsky, A.; Pankov, R.; Yamada, K. M. *Nat. Rev. Mol. Cell Biol.* **2001**, *2* (11), 793–805.
(2) Geiger, B.; Spatz, J. P.; Bershadsky, A. D. *Nat. Rev. Mol. Cell Biol.* **2009**, *10* (1), 21–33.
(3) Clark, E. A.; Brugge, J. S. *Science* **1995**, *268* (5208), 233–239.
(4) Giancotti, F. G.; Ruoslahti, E. *Science* **1999**, *285* (5430), 1028–1032.
(5) Cohen, M.; Joester, D.; Geiger, B.; Addadi, L. *Chembiochem* **2004**, *5* (10), 1393–1399.
(6) Zimerman, B.; Volberg, T.; Geiger, B. *Cell Motil. Cytoskeleton* **2004**, *58* (3), 143–159.
(7) Yurchenco, P. D.; Cheng, Y. S.; Campbell, K.; Li, S. H. *J. Cell Sci.* **2004**, *117* (5), 735–742.
(8) Arnold, M.; Cavalcanti-Adam, E. A.; Glass, R.; Blummel, J.; Eck, W.; Kantlehner, M.; Kessler, H.; Spatz, J. P. *ChemPhysChem* **2004**, *5* (3), 383–388.
(9) Cavalcanti-Adam, E. A.; Micoulet, A.; Blummel, J.; Auernheimer, J.; Kessler, H.; Spatz, J. P. *Eur. J. Cell Biol.* **2006**, *85* (3−4), 219–224.
(10) Huang, J. H.; Grater, S. V.; Corbellinl, F.; Rinck, S.; Bock, E.; Kemkemer, R.; Kessler, H.; Ding, J. D.; Spatz, J. P. *Nano Lett.* **2009**, *9* (3), 1111–1116.
(11) Arnold, M.; Schwieder, M.; Blummel, J.; Cavalcanti-Adam, E. A.; Lopez-Garcia, M.; Kessler, H.; Geiger, B.; Spatz, J. P. *Soft Matter* **2009**, *5* (1), 72–77.
(12) Wolfram, T.; Spatz, J. P.; Burgess, R. W. *BMC Cell Biol.* **2008**, 9.
(13) Cavalcanti-Adam, E. A.; Aydin, D.; Hirschfeld-Warneken, V. C.; Spatz, J. P. *HFSP J.* **2008**, *2* (5), 276–285.
(14) Arnold, M.; Hirschfeld-Warneken, V. C.; Lohmuller, T.; Heil, P.; Blummel, J.; Cavalcanti-Adam, E. A.; Lopez-Garcia, M.; Walther, P.; Kessler, H.; Geiger, B.; Spatz, J. P. *Nano Lett.* **2008**, *8* (7), 2063–2069.
(15) Chen, C. S.; Mrksich, M.; Huang, S.; Whitesides, G. M.; Ingber, D. E. *Science* **1997**, *276* (5317), 1425–1428.
(16) Justesen, J.; Lorentzen, M.; Andersen, L. K.; Hansen, O.; Chevallier, J.; Modin, C.; Fuchtbauer, A.; Foss, M.; Besenbacher, F.; Duch, M.; Pedersen, F. S. *J. Biomed. Mater. Res., Part A* **2009**, *89A* (4), 885–894.
(17) Feinberg, A. W.; Wilkerson, W. R.; Seegert, C. A.; Gibson, A. L.; Hoipkemeier-Wilson, L.; Brennan, A. B. *J. Biomed. Mater. Res., Part A* **2008**, *86A* (2), 522–534.
(18) Flemming, R. G.; Murphy, C. J.; Abrams, G. A.; Goodman, S. L.; Nealey, P. F. *Biomaterials* **1999**, *20* (6), 573–588.
(19) Gallant, N. D.; Michael, K. E.; Garcia, A. J. *Mol. Biol. Cell* **2005**, *16* (9), 4329–4340.
(20) Steinberg, T.; Schulz, S.; Spatz, J. P.; Grabe, N.; Mussig, E.; Kohl, A.; Komposch, G.; Tomakidi, P. *Nano Lett.* **2007**, *7* (2), 287–294.
(21) Lehnert, D.; Wehrle-Haller, B.; David, C.; Weiland, U.; Ballestrem, C.; Imhof, B. A.; Bastmeyer, M. *J. Cell Sci.* **2004**, *117* (1), 41–52.
(22) Pesen, D.; Haviland, D. B. *ACS Appl. Mater. Interfaces* **2009**, *1* (3), 543–548.
(23) Slater, J. H.; Frey, W. *J. Biomed. Mater. Res., Part A* **2008**, *87A* (1), 176–195.
(24) Hanarp, P.; Sutherland, D. S.; Gold, J.; Kasemo, B. *Colloids Surf., A* **2003**, *214* (1−3), 23–36.
(25) Agheli, H.; Malmstrom, J.; Larsson, E. M.; Textor, M.; Sutherland, D. S. *Nano Lett.* **2006**, *6* (6), 1165–1171.
(26) Malmstrom, J.; Agheli, H.; Kingshott, P.; Sutherland, D. S. *Langmuir* **2007**, *23* (19), 9760–9768.
(27) Goodwin, A. E.; Pauli, B. U. *J Immunol. Methods* **1995**, *187* (2), 213–219.
(28) Shroff, H.; Galbraith, C. G.; Galbraith, J. A.; Betzig, E. *Nat. Methods* **2008**, *5* (5), 417–423.
(29) Burridge, K.; Fath, K.; Kelly, T.; Nuckolls, G.; Turner, C. *Ann. Rev. Cell Biol.* **1988**, *4*, 487–525.
(30) Cramer, L.; Mitchison, T. J. *J. Cell Biol.* **1993**, *122* (4), 833–843.
(31) Lauffenburger, D. A.; Horwitz, A. F. *Cell* **1996**, *84* (3), 359–369.
(32) Rid, R.; Schiefermeier, N.; Grigoriev, I.; Small, J. V.; Kaverina, I. *Cell Motil. Cytoskeleton* **2005**, *61* (3), 161–171.
(33) Discher, D. E.; Janmey, P.; Wang, Y. L. *Science* **2005**, *310* (5751), 1139–1143.
(34) Solon, J.; Levental, I.; Sengupta, K.; Georges, P. C.; Janmey, P. A. *Biophys. J.* **2007**, *93* (12), 4453–4461.
(35) Dalby, M. J.; Gadegaard, N.; Tare, R.; Andar, A.; Riehle, M. O.; Herzyk, P.; Wilkinson, C. D. W.; Oreffo, R. O. C. *Nat. Mater.* **2007**, *6* (12), 997–1003.
(36) Berry, C. C.; Curtis, A. S. G.; Oreffo, R. O. C.; Agheli, H.; Sutherland, D. S. *IEEE Trans. Nanobiosci.* **2007**, *6* (3), 201–209.
(37) Garcia, A. J.; Vega, M. D.; Boettiger, D. *Mol. Biol. Cell* **1999**, *10* (3), 785–798.
(38) Erickson, H. P. *Proc. Natl. Acad. Sci. U.S.A.* **1994**, *91* (21), 10114–10118.
(39) Balaban, N. Q.; Schwarz, U. S.; Riveline, D.; Goichberg, P.; Tzur, G.; Sabanay, I.; Mahalu, D.; Safran, S.; Bershadsky, A.; Addadi, L.; Geiger, B. *Nat. Cell Biol.* **2001**, *3* (5), 466–472.
(40) Andersson, A. S.; Backhed, F.; von Euler, A.; Richter-Dahlfors, A.; Sutherland, D.; Kasemo, B. *Biomaterials* **2003**, *24* (20), 3427–3436.
(41) Dalby, M. J.; Riehle, M. O.; Sutherland, D. S.; Agheli, H.; Curtis, A. S. G. *Biomaterials* **2004**, *25* (23), 5415–5422.

DOI: 10.1021/nl903875r | *Nano Lett.* **XXXX,** *xxx,* 000-000